Optimization of HDR brachytherapy dose distributions using linear programming with penalty costs

Ron Alterovitz[a)]
Department of Industrial Engineering and Operations Research, University of California, Berkeley, 4141 Etcheverry Hall, Berkeley, California 94720-1777

Etienne Lessard, Jean Pouliot, and I-Chow Joe Hsu
Department of Radiation Oncology, University of California, San Francisco, Comprehensive Cancer Center, 1600 Divisadero Street, Suite H1031, San Francisco, California 94143-1708

James F. O'Brien
Department of Electrical Engineering and Computer Science, University of California, Berkeley, 633 Soda Hall, Berkeley, California 94720-1776

Ken Goldberg
Department of Industrial Engineering and Operations Research and Department of Electrical Engineering and Computer Science, University of California, Berkeley, 4141 Etcheverry Hall, Berkeley, California 94720-1777

(Received 14 January 2006; revised 27 July 2006; accepted for publication 2 August 2006; published 9 October 2006)

Prostate cancer is increasingly treated with high-dose-rate (HDR) brachytherapy, a type of radiotherapy in which a radioactive source is guided through catheters temporarily implanted in the prostate. Clinicians must set dwell times for the source inside the catheters so the resulting dose distribution minimizes deviation from dose prescriptions that conform to patient-specific anatomy. The primary contribution of this paper is to take the well-established dwell times optimization problem defined by Inverse Planning by Simulated Annealing (IPSA) developed at UCSF and exactly formulate it as a linear programming (LP) problem. Because LP problems can be solved exactly and deterministically, this formulation provides strong performance guarantees: one can rapidly find the dwell times solution that globally minimizes IPSA's objective function for any patient case and clinical criteria parameters. For a sample of 20 prostates with volume ranging from 23 to 103 cc, the new LP method optimized dwell times in less than 15 s per case on a standard PC. The dwell times solutions currently being obtained clinically using simulated annealing (SA), a probabilistic method, were quantitatively compared to the mathematically optimal solutions obtained using the LP method. The LP method resulted in significantly improved objective function values compared to SA ($P=1.54\times10^{-7}$), but none of the dosimetric indices indicated a statistically significant difference ($P<0.01$). The results indicate that solutions generated by the current version of IPSA are clinically equivalent to the mathematically optimal solutions. © *2006 American Association of Physicists in Medicine*. [DOI: 10.1118/1.2349685]

Key words: HDR, optimization, conformal radiotherapy, prostate therapy, IPSA

I. INTRODUCTION

Prostate cancer, which kills an estimated 30 000 Americans each year,[1] is increasingly treated with high-dose-rate (HDR) brachytherapy, a medical procedure in which radioactive sources are guided through catheters to provide a high radioactive dose to the cancer while sparing surrounding healthy tissues. In HDR brachytherapy, the physician commonly implants 14–18 catheters in the prostate through the perineum under ultrasound guidance. The catheters are attached to an HDR Remote Afterloader for treatment delivery. The afterloader moves a single radioactive source, typically 4.5 mm long and 0.9 mm in diameter containing ^{192}Ir, inside each catheter, stopping temporarily at predetermined dwell locations. By adjusting the length of time (dwell time) that the source remains at any location within a catheter (dwell position), it is possible to generate a wide variety of dose distributions.

When treating prostate cancer, physicians desire dose distributions that conform to patient anatomy and satisfy dose prescriptions for the target volume (prostate) and nearby critical organs (urethra, bladder, and rectum).[2] Prior to connecting the afterloader, the physician obtains an image (usually CT scan or MRI) of the catheters, prostate, and surrounding tissues and prescribes clinical dose requirements for each tissue type. The goal is then to select dwell times to satisfy the clinical criteria as best as possible. This goal can be formulated as an optimization problem: compute dwell times to minimize deviation from prescribed dose subject to dwell position and dose feasibility constraints.

To address this optimization problem, Lessard and Pouliot developed Inverse Planning by Simulated Annealing (IPSA).[3–5] IPSA has been used in the treatment planning of over a thousand patients at UCSF since 2000 and has been independently evaluated by different American and European institutions.[6–11]

A complete description of IPSA and its clinical applications was recently published.[12] Only the elements required for the present work are described here. Using hand-segmented boundaries of the prostate, urethra, bladder, and rectum, and often the penile bulb and dominant intraprostatic lesions,[13] the software generates a discrete sample of dose calculation points inside and on the boundary of the tissue types. For dose calculation points of each tissue type, IPSA permits the physician to prescribe unique dose ranges as well as penalty costs that grow linearly when actual dose violates the prescribed dose ranges. Setting dwell times to minimize dose penalty costs rather than using rigid dose constraints guarantees that the method will find an achievable solution. IPSA defines an objective function equal to a weighted sum of penalty costs at dose calculation points given the dwell times. In the IPSA framework, the mathematically optimal solution is the solution of dwell times that globally minimizes the objective function. IPSA's single objective function assumes that the clinician has specified desirable dose penalty costs and generates a single dwell times solution, in contrast to multiobjective optimization formulations that consider the weights as variables and generate a Pareto front of solutions.[14,15]

The current version of IPSA software uses simulated annealing (SA) to compute dwell times to minimize the objective function. The computation time for a typical case is about 10 s on PC with a 3.6 GHz Intel Xeon processor (Nucletron's Masterplan Station). The computation time includes the automatic selection of the active dwell positions, the generation of the dose calculation points, the generation of a look-up dose-rate table, and 100 000 simulated annealing iterations. SA applies a random search with the ability to escape local minima and offers a statistical guarantee to converge asymptotically to the global minimum.[16–18] The longer the SA algorithm searches for a solution, the higher the probability that the optimal solution is found. Although this method has worked well in clinical practice using 100 000 iterations, there previously was no general quantitative information available regarding the closeness to mathematical optimality of the solutions obtained using simulated annealing, a probabilistic method that cannot guarantee the achievement of a global minimum within a finite computation time.

Our primary contribution is to take the well-established dose optimization problem defined by IPSA and show that it can be exactly formulated as a linear programming (LP) problem. Because the global minimum for a LP problem can be computed exactly and deterministically using preexisting algorithms, this formulation provides strong performance guarantees for cost minimization: one can rapidly find the minimum cost solution for any patient case and clinical criteria parameters. LP does not require setting parameters specific to the optimization method, such as stopping criteria or pseudo-temperatures for SA or mutation probabilities for GA.[14,19,15] This allows clinicians to customize dose prescriptions and penalty costs based on medical considerations without concern about their effect on the convergence of the optimization method. Unlike other deterministic algorithms such as local search,[3] the LP method will never be trapped at sub-optimal solutions of IPSA's objective function. Since the LP solution is guaranteed to globally minimize the objective function, it provides a precise baseline for evaluating solutions currently being obtained clinically by probabilistic methods such as SA.

Our second contribution is to compare quantitatively the solutions for HDR dwell times obtained by SA, current clinical practice, with the mathematically optimal solutions obtained using LP. With a sample of 20 prostate cancer patient cases, we show that the LP method resulted in significantly improved objective function values compared to SA, but the dose distributions produced by the dwell times solutions were clinically equivalent as measured by standard dosimetric indices.

A linear programming problem is defined by an objective function and constraints that are linear functions of the variables. A LP problem can be solved using the SIMPLEX algorithm, a global deterministic optimization method that considers the geometric polyhedron defined by the linear constraints and systematically moves along edges of the polyhedron to new feasible solutions (represented as vertices of the polyhedron) with successively better values of the objective function until the optimum is reached.[20] In 1990, Renner *et al.* was the first group to propose a linear programming formulation for HDR brachytherapy dose optimization. Their method minimizes the time the source is irradiating tissue subject to a minimum dose constraint for a set of points in the target volume.[21] Kneschaurek *et al.* extended this method to permit the specification of dose ranges using rigid constraints for both minimum and maximum dose.[22] Jozsef *et al.* also used rigid constraints on dose range and minimized the maximum deviation from a prescribed dose constant at dose calculation points.[23] However, a solution of dwell times that results in a dose distribution that satisfies the rigid constraints may not be physically realizable. By defining the dwell times as variables and defining rigid linear constraints on dose, these previous approaches formulated the LP problem in a manner that does not guarantee the output of a solution since no feasible solution may exist. Finding a clinically realizable solution in such cases necessitates arbitrarily removing some rigid dose constraints, which requires substantial human intervention.

Our new LP formulation combines the advantages of IPSA's cost functions and extensive clinical validation with the benefits of deterministic global optimization for cost minimization. We show that the new LP method computes in finite time the mathematically optimal solution for dwell times to generate the best achievable dose distribution given the clinical objectives and the preoptimization data generated by IPSA (active dwell positions, dose calculation points, and dose rate look-up table). We applied both SA and the new LP

method to 20 prostate cancer patient cases and evaluated improvement of results using objective function values and standard dosimetric indices.

II. METHODS AND MATERIALS

A. Patient data sets

We applied the LP method retrospectively to 20 prostate cancer patient cases. The prostate volumes ranged from 23 to 103 cc. For these patients, the physician implanted 14–18 catheters in the prostate with transrectal ultrasound (TRUS) guidance while the patient was under epidural anesthesia. Then Flexi-guide catheters (Best Industries, Inc., Flexi-needles, 283-25 (FL153-15NG)), which are 1.98-mm-diam hollow plastic needles through which the radioactive source will move, were inserted transperineally by following the tip of the catheter from the apex of the prostate to the base of the prostate using ultrasound and a stepper. A Foley catheter was inserted to help visualize the urethra.

After catheter implantation, a treatment planning pelvic CT scan was obtained for each patient. Three-millimeter-thick CT slices were collected using a spiral CT. The clinical target volume (CTV) and critical organs (COs) including bladder, rectum, and urethra were contoured using the Nucletron Plato Version 14.2.6 (Nucletron B.V., Veenendaal, The Netherlands). The CTV included only the prostate and no margin was added. When segmenting the bladder and rectum, the outermost mucosa surface was contoured. The urethra was defined by the outer surface of the Foley catheter. Only the urethral volume within the CTV was contoured. The COs were contoured on all CT slices containing the CTV and at least two additional slices above and below. Implanted catheters were also segmented.

From the segmented anatomical structures, IPSA selected the active dwell positions and generated a set of m dose calculation points for which the optimization methods will calculate dose. The dose calculation points are distributed based on the anatomy and the implant in order to represent an accurate measurement of the clinical objectives.[5] For the 20 cases, m ranged from 1781 to 3510. Since the selection of the active dwell positions and dose calculation points affects the outcome of optimization,[24] we use those generated by IPSA as input for the LP method. For each contoured volume, IPSA uses two categories of dose calculation points: "surface" and "volume." This results in 8 dose calculation point types: "surface" and "volume" for the four contoured tissue types (prostate, urethra, bladder, and rectum). For each tissue type, adjusting the dose to "surface" dose calculation points controls the dose coverage and conformality while adjusting the dose to "volume" dose calculation points controls the dose homogeneity.[2]

All patients were treated at UCSF Comprehensive Cancer Center using dosimetric plans generated by the current version of IPSA. We used imaging and dosimetry records from those treatments to compare SA with LP.

TABLE I. Clinical criteria parameters for dose penalty cost functions.

s	Dose calculation point type	$D_s^{\min}$ (cGy)	$M_s^{\min}$	$D_s^{\max}$ (cGy)	$M_s^{\max}$
1	Prostate (surface)	950	100	1425	100
2	Prostate (volume)	950	100	1425	30
3	Urethra (surface)	950	100	1140	30
4	Urethra (volume)	950	100	1140	30
5	Rectum (surface)	0	0	475	20
6	Rectum (volume)	0	0	475	20
7	Bladder (surface)	0	0	475	20
8	Bladder (volume)	0	0	475	20

B. Dose calculation

Dwell positions are defined as points along catheters at which a source can be placed for a nonzero interval of time. The n active dwell positions were selected by IPSA. We define the dwell time of a source at dwell position j by t_j. A dwell time of 0 corresponds to skipping past a dwell position. The dwell times t_j are the variables that will be set to produce a dose distribution that satisfies the clinical criteria as best as possible.

We calculate the dose-rate contribution d_{ij} of a dwell position j to a dose calculation point i as specified in the AAPM TG-43 dosimetry protocol.[25,26] The dose-rate contribution is a function of r_{ij}, the distance between the dwell position j and the dose calculation point i. It also depends on the radioactive material used in the source, which was ^{192}Ir. Since small differences in the dose calculation may affect the outcome of the optimization, we use the look-up dose-rate table calculated by IPSA as an input for the LP method.

The dose contribution of a dwell position j to a dose calculation point i is computed by multiplying the dose-rate contribution d_{ij} by the dwell time t_j. The dose D_i at a dose calculation point i, which has units of cGy, is calculated by summing the dose contribution from each dwell position,

$$D_i = \sum_{j=1}^{n} d_{ij} t_j.$$

C. Clinical criteria

After contouring, the physician prescribes dose ranges for each anatomical structure. The dose ranges used in this study, listed in Table I, are typical values clinically used at the UCSF Comprehensive Cancer Center.[2] This includes the minimum dose $D_s^{\min}$ and maximum dose $D_s^{\max}$ for each dose calculation point type s. For a dose calculation point i of type s, the desired dose D_{si} should satisfy $D_s^{\min} \leqslant D_{si} \leqslant D_s^{\max}$.

In practice, it may not be physically possible to provide a radioactive dose in the physician specified range for every dose calculation point in the three-dimensional volume. Hence, the physician also specifies a "penalty" for any point for which the clinical criteria is not satisfied. If the actual dose is below or above the prescribed range, the penalty increases linearly at rates $M_s^{\min}$ and $M_s^{\max}$, respectively. Adjustment of $M_s^{\min}$ and $M_s^{\max}$ sets the relative importance of

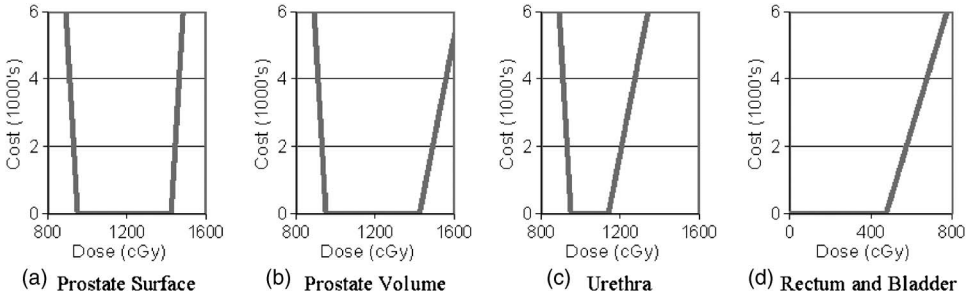

FIG. 1. The clinical criteria are specified using cost functions which define penalty as a function of dose for the each dose calculation point type.

dose range satisfaction between anatomical structures. The penalty weights $M_s^{\min}$ and $M_s^{\max}$ used in this study, listed in Table I, are typical values used at the UCSF Comprehensive Cancer Center.[2] The penalty w_{si} at a dose calculation point i of type s can be described in mathematical form using a cost function,

$$w_{si} = \begin{cases} -M_s^{\min}(D_{si} - D_s^{\min}) & \text{if } D_{si} \leqslant D_s^{\min} \\ M_s^{\max}(D_{si} - D_s^{\max}) & \text{if } D_{si} \geqslant D_s^{\max} \\ 0 & \text{if } D_s^{\min} < D_{si} < D_s^{\max}. \end{cases} \quad (1)$$

Figure 1 plots the cost functions (penalty as a function of dose) for the clinical criteria in Table I.

D. Linear programming formulation

The objective is to satisfy the clinical criteria as best as possible by computing dwell times that minimize the net dose penalty costs. Equation (1) from Sec. II C defines the cost function for an individual dose calculation point i of type s based on the clinical criteria for that point. For each type s, we define the penalty cost E_s as the average penalty cost per point:

$$E_s = \sum_{i=1}^{m_s} \frac{w_{si}}{m_s}, \quad (2)$$

where m_s is the number of dose calculation points of type s. The objective function E is effectively a weighted sum of the average cost for each tissue type s, where the relative weights are determined by the costs $M_s^{\min}$ and $M_s^{\max}$. The global objective function is to minimize the sum of the penalty costs for the eight dose calculation point types:

$$E = \sum_{s=1}^{8} E_s = \sum_{s=1}^{8} \sum_{i=1}^{m_s} \frac{w_{si}}{m_s}. \quad (3)$$

This objective function is identical to the objective function used by IPSA.[3]

The objective function E is not linear because it is composed of nonlinear functions w_{si}. However, each function w_{si} is piece-wise linear. We can formulate this problem as a linear program by creating artificial variables c_{si} to represent cost and defining the following constraints:

$$c_{si} \geqslant -M_s^{\min}(D_{si} - D_s^{\min}),$$

$$c_{si} \geqslant M_s^{\max}(D_{si} - D_s^{\max}),$$

$$c_{si} \geqslant 0. \quad (4)$$

Because w_{si} is a piece-wise linear and convex function, the above-noted constraints guarantee that $c_{si} \geqslant w_{si}$ for all i, s. Furthermore, we redefine the global objective function to

$$E = \sum_{s=1}^{8} \sum_{i=1}^{m_s} \frac{c_{si}}{m_s}.$$

For minimized E where the costs c_{si} satisfy the inequalities (4), we are guaranteed $c_{si} = w_{si}$ for all s, i. We show this by proving the contrapositive ($c_{si} \neq w_{si}$ implies E not minimized), which is logically equivalent.[27] If $c_{si} \neq w_{si}$, then $c_{si} > w_{si}$ for some s, i and there will exist a cost c'_{si} such that $c_{si} > c'_{si} \geqslant w_{si}$. Since c'_{si} will not violate any constraint in inequalities (4), it is feasible. We define E' exactly as E except using c'_{si} instead of c_{si}. Hence, $E' < E$ and no cost variables used to compute E' violate a constraint, which implies E is not minimized. Hence, for minimized E, we are guaranteed $c_{si} = w_{si}$.

We explicitly define the linear program in canonical form[20] by plugging into the constraints the dose distribution D_{si} at point i of type s due to dwell times t_j.

Minimize

$$E = \sum_{s=1}^{8} \sum_{i=1}^{m_s} \frac{c_{si}}{m_s}.$$

Subject to

$$\begin{aligned} & c_{si} + \sum_{j=1}^{n} M_s^{\min} d_{sij} t_j \geqslant M_s^{\min} D_s^{\min}, && s = 1, \ldots, 8; i = 1, \ldots, m_s, \\ & c_{si} - \sum_{j=1}^{n} M_s^{\max} d_{sij} t_j \geqslant -M_s^{\max} D_s^{\max}, && s = 1, \ldots, 8; i = 1, \ldots, m_s, \\ & c_{si} \geqslant 0, && s = 1, \ldots, 8; i = 1, \ldots, m_s, \\ & t_j \geqslant 0, && j = 1, \ldots, n. \end{aligned} \quad (5)$$

Because of the properties of the artificial variables c_{si} shown earlier for minimized E, the optimal solution obtained for the linear program will be the same as the optimal solution to the nonlinear formulation based on the objective function in Eq. (3) with the cost functions in Eq. (1). We effectively transformed the nonlinear IPSA optimization problem in Eq. (3) (for which deterministic optimization algorithms such as local search could be trapped at sub-optimal solutions[3]) to a

higher dimensional space with artificial variables in which an equivalent linear formulation (5) can be minimized deterministically to find the global optimal solution using the SIMPLEX algorithm.

E. Method evaluation

We implemented software using C++ to read patient specific parameters from IPSA and output the linear program (5) in the file format of AMPL (A Mathematical Programming Language).[28] We solved the linear program specified in each AMPL file using ILOG CPLEX 9.0, an advanced implementation of the SIMPLEX algorithm[20] designed for large industrial optimization problems.[29] Computation was performed on a 3.0 GHz Pentium IV computer running the Linux operating system.

We recorded the dwell times and the objective function value E for the solutions obtained using SA and LP. We evaluated the resulting dose distributions using standard dosimetric indices, including prostate V100 and V150 (the percentage of the prostate receiving over 100% and over 150% of the prescribed dose, respectively). As dose inside the prostate should fall between 100% ($D^{\min}$) and 150% ($D^{\max}$) of prescribed dose, ideally V100 should be 100% and V150 should be 0%. Similarly, we also evaluated V100 and V150 for the urethra. Dosimetric indices for normal structures (noncancerous tissues) include the rectum (V50 and V100) and the bladder (V50 and V100). As normal structures should be spared radioactive dose, these indices ideally should be close to 0%. We also computed dosimetric indices in absolute dose, including the prostate D90 (the maximal dose that covers 90% of prostate volume), urethra D10 (the maximal dose that covers 10% of urethra volume), and rectum and bladder D2cc (the maximal dose that covers 2cc of the organ volume).

III. RESULTS

ILOG CPLEX solved for the optimal solution to the linear programming formulation in an average time of 9.00 s per case with a standard deviation of 3.77 s for the 20 prostate cancer patient cases. The times ranged from 3.68 to 14.63 s. The SIMPLEX algorithm in ILOG CPLEX required an average of 1653 iterations with a standard deviation of 341 iterations.

The average objective function value for the 20 prostate cancer patient cases was 3.27 for the LP method compared to 3.33 for SA. The percent difference in objective function value between the solution found using SA and the optimal solution found using LP for each individual patient case is shown in Fig. 2. Improvement varies from a minimum of 0.84% to a maximum of 4.59%. We performed paired t-tests to determine the statistical significance ($P<0.01$) of the results and found that the improvement in objective function value using the LP method compared to SA was statistically significant ($P=1.54\times10^{-7}$).

Figure 3 displays the standard dosimetric indices for both the SA and LP solutions. The bars indicate the mean indices as percents and the error bars indicate the maximum and minimum indices obtained for the 20 prostate cancer patient cases. Based on these dosimetric indices, the difference between the dose distributions generated by SA and LP was small. None of the dosimetric indices indicated a statistically significant ($P<0.01$) difference between the dose distributions generated by SA and LP. The largest improvement for the prostate D90, the rectum D2cc, and the bladder D2cc were lower than 1%. The largest improvement for the urethra D10 was 2%. The urethra V150 was zero for both LP and SA method for this case. Additional dosimetic indices are shown in Table II where positive values indicate improvement and negative values indicate deterioration. The deterioration of one dosimetric index is sometimes traded for the improvement of other dosimetric indices and the improvement of the global solution. The maximum improvement of LP over SA

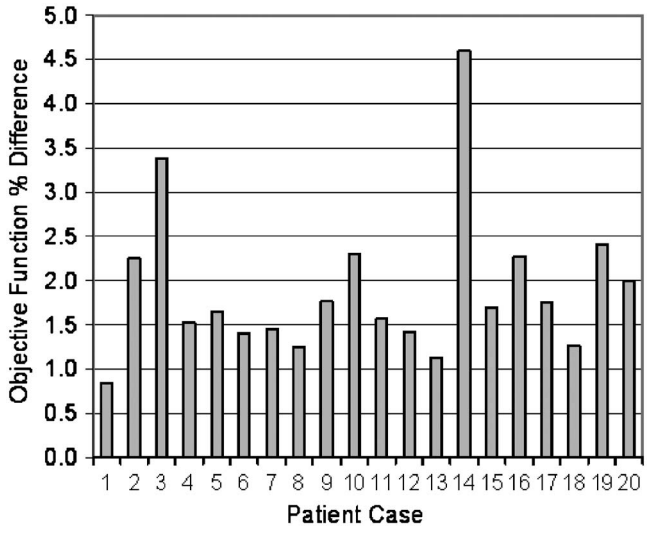

FIG. 2. The percent difference in objective function value between the optimal solution (found using the LP method) and the solution found by SA for 20 prostate cancer patient cases. The difference is statistically significant ($P=1.54\times10^{-7}$).

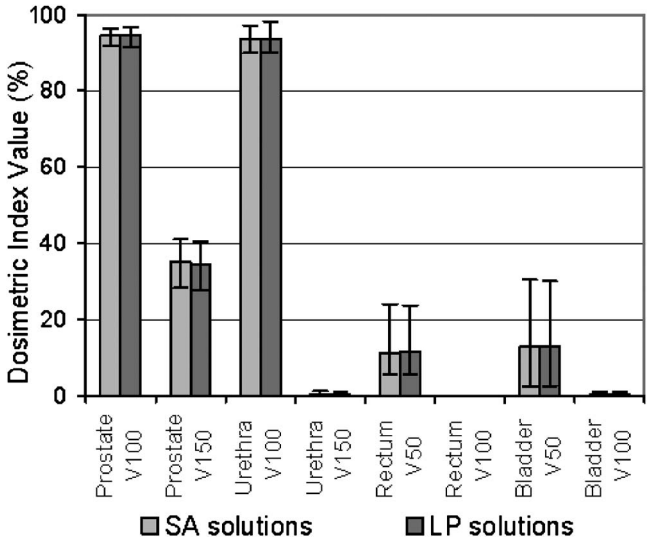

FIG. 3. Mean dosimetric index results for the SA and LP methods for 20 prostate cancer patient cases. Error bars indicate maximum and minimum values for the 20 patient cases.

TABLE II. Improvement of LP solutions over SA solutions for 20 prostate cancer patient cases calculated as the absolute difference in dosimetric index percent values. Negative values indicate deterioration in the dosimetric index. The significance P of the differences was computed using paired t-tests.

Dosimetric index	Maximum improvement	Minimum improvement	Mean improvement	99% CI	Significance P
Prostate V100	0.95	−0.49	0.13	(−0.10, 0.37)	0.1644
Prostate V150	1.65	−1.63	0.51	(−0.02, 1.04)	0.0217
Urethra V100	1.52	−1.50	0.12	(−0.33, 0.57)	0.4858
Urethra V150	0.11	−0.05	0.00	(−0.01, 0.02)	0.7621
Rectum V50	0.50	−0.81	−0.17	(−0.36, 0.02)	0.0344
Rectum V100	0.03	0.00	0.01	(−0.00, 0.01)	0.0289
Bladder V50	0.75	−0.48	0.03	(−0.17, 0.23)	0.7042
Bladder V100	0.13	−0.02	0.02	(−0.00, 0.04)	0.0225

was a reduction of 1.65% for the prostate V150 index. However, for the same patient, LP resulted in a reduction of 0.38% of the prostate V100. Similarly, the maximum deterioration of LP over SA was an increase of 1.63% for the prostate V150 index inducing an improvement of 0.84% of the prostate V100. Even with these two extreme cases, the LP and SA methods provide two different solutions that are difficult to distinguish clinically. Figure 4 plots the dose-volume-histogram (DVH) for each tissue type for the patient case with the greatest magnitude improvement in a dosimetric index between the SA and LP solutions. Figure 5 displays a CT scan of the same patient with overlaid isodose contours for both solutions.

IV. DISCUSSION

The dosimetric index results are not significantly different from those of the current version of IPSA, which was previously shown to be superior to the commonly used method of geometric optimization followed by manual adjustment.[2,6]

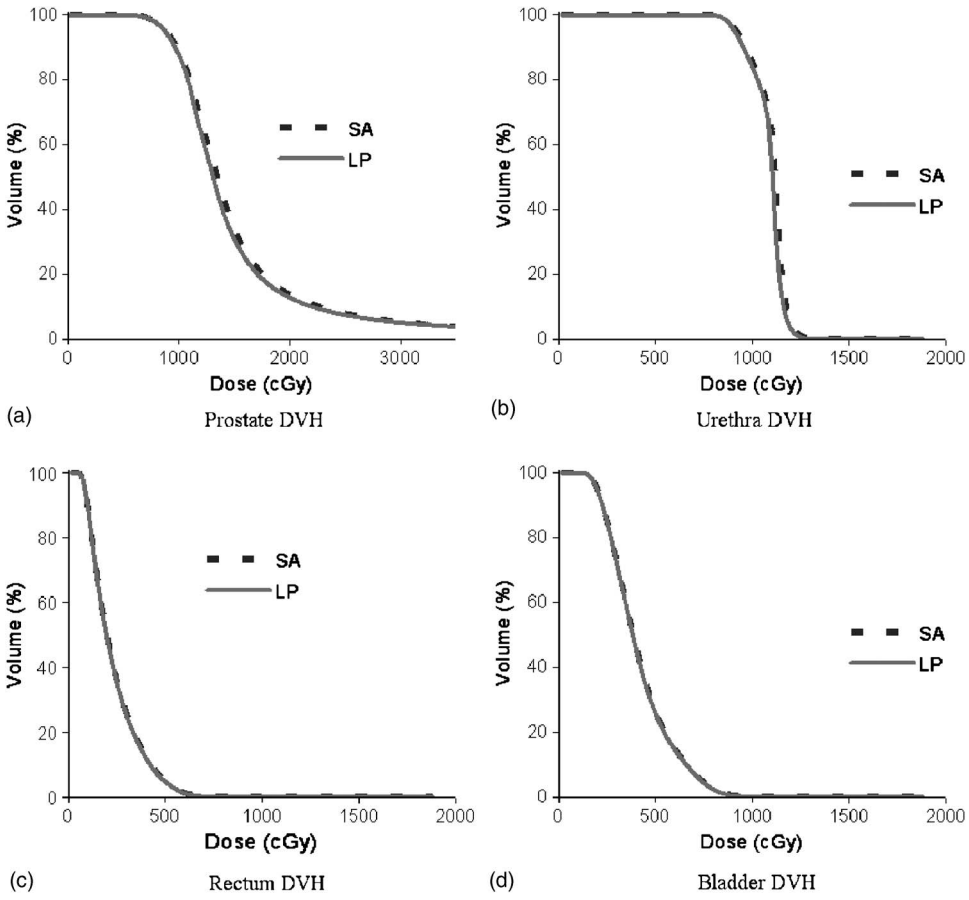

FIG. 4. DVH plots for the prostate (a), urethra (b), rectum (c), and bladder (d) for the patient case with greatest difference in dosimetric indices between the LP and SA solutions. For dose less than D^{min} for each tissue type, the desired volume is 100%. For dose greater than D^{max}, the desired volume 0%.

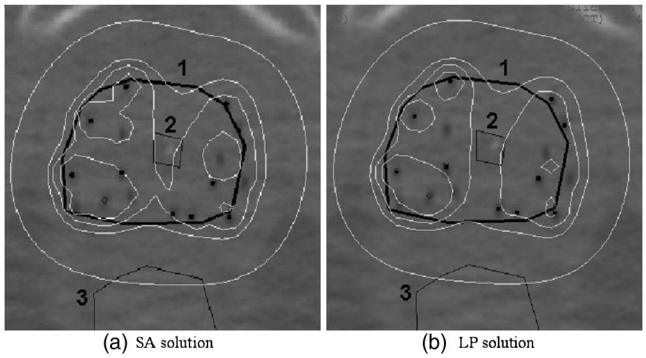

FIG. 5. Isodose curves for the SA (a) and LP (b) solutions for the patient case with greatest difference in dosimetric indices. The prostate (1), urethra (2), and rectum (3) are contoured in black. Catheters are shown as black dots. Isodose curves for 50%, 100% ($D^{\min}$), 120%, and 150% ($D^{\max}$) of prostate minimum prescribed dose are plotted in white.

The small variances observed for the prostate and urethra in Fig. 3 show the consistency of the treatment plan quality for both the SA and LP methods. The larger variances for the prostate V150, the rectum, and the bladder are due to differences between patients in anatomy, prostate volume, and distances between the prostate and organs at risk.

The LP and SA methods are both based on IPSA's objective function for the HDR brachytherapy dwell time optimization problem. The only difference is the optimization algorithm used, simulated annealing versus an equivalent linear programming formulation that can be solved using the SIMPLEX algorithm. As simulated annealing is a probabilistic method, it is only guaranteed to converge to an optimal solution after an infinite amount of computation time. Standard termination criteria, such as stopping the algorithm after a fixed number of iterations, can result in suboptimal solutions. During the development phase of the current version of IPSA, a large number of cases were run using a very large number of iterations (>1 million) and no significant improvements in the dosimetric indices were found compared to the values found after 100 000 iterations. However, the closeness to mathematical optimality of the solutions of the current version of IPSA could not be guaranteed for every new clinical case.

Because the LP formulation of IPSA's objective function can be solved deterministically to find the solution that globally minimizes costs, the LP method solution provides a precise baseline for evaluating solutions obtained by probabilistic methods such as SA. The LP method computed a solution with a better objective function value compared to SA for every patient case. The improvement in objective function values of LP compared to SA was statistically significant. However, the effect size of the objective function improvement was not sufficient to result in statistically significant differences in standard dosimetric indices for our sample of 20 prostates with volume ranging from 23 to 103 cc. We observe that the DVH plots for the patient case with the largest difference in dosimetric indices are similar for both methods (Fig. 4) while differences are observable on the isodose curves (Fig. 5). The hot spots (prostate V150) have different shapes and the prostate V120 curve is at a different location. This indicates that the local dose distribution (isodose) is different while global dose delivered to the organs (DVH) and critical dose delivered to the organs (dosimetric indices) are equivalent. This quantitatively indicates that the dose distributions generated by SA are clinically equivalent to the best achievable dose distributions based on the current IPSA objective function with dose constraints and penalty weights selected for prostate cancer cases.

V. CONCLUSION

Prostate cancer is increasingly treated with HDR brachytherapy, a type of radiotherapy in which a radioactive source is guided through catheters temporarily implanted in the prostate. Clinicians must set dwell times for the source inside the catheters so the resulting dose distribution minimizes deviation from dose prescriptions that conform to patient-specific anatomy. The primary contribution of this paper is to take the well-established dwell times optimization problem defined by IPSA developed at UCSF and exactly formulate it as a LP problem. Because LP problems can be solved exactly and deterministically, this formulation provides strong performance guarantees: one can rapidly find the dwell times solution that globally minimizes IPSA's objective function for any patient case and clinical criteria parameters. For a sample of 20 prostate cancer patient cases, the new LP method optimized dwell times in less than 15 s per case on a standard PC.

We quantitatively compared the dwell times solutions currently being obtained clinically using SA, a probabilistic method, to the mathematically optimal solutions obtained using the LP method. The LP method resulted in significantly improved objective function values compared to SA, but none of the dosimetric indices indicated a statistically significant difference. The results indicate that solutions generated by the current version of IPSA are clinically equivalent to the mathematically optimal solutions.

IPSA's objective function with dose constraints and penalty weights covers all organs and all clinical objectives so they can be optimized simultaneously. The physician can adjust the objectives for each optimization. However, if a particular set of objectives generates the desired results then the same set of objectives can be used for optimization of clinically similar cases (i.e., prostate) without further adjustments. This set of objectives, commonly called a class solution, can be used as a starting point for every patient, significantly reducing the time needed to plan individual patient treatments.

Our linear programming formulation was designed for prostate cancer patient cases. The mathematical formulation can be extended to other cancer types for which HDR brachytherapy is used by incorporating different clinical parameters, although integrating and testing the LP method with medical imaging and segmentation for other cancer types would require substantial effort. The method can also be extended to support any piece-wise linear convex cost

functions, not solely the three-piece cost functions presented earlier. Recent developments in magnetic resonance spectroscopy imaging and image registration introduce a new clinical criterion, a dose boost to the tumor volume within the prostate.[30–32] Although we do not explicitly consider that dose calculation point type, the mathematical formulation we defined can be extended to incorporate it by adding a tumor volume tissue type. A potential advantage of the LP method for each of these extensions is that it will use the well-established framework of IPSA and deterministically compute mathematically optimal dwell time solutions for all patient cases.

ACKNOWLEDGMENTS

This work was supported in part by the National Institutes of Health under Grant No. R21 EB003452 and by a National Science Foundation Graduate Research Fellowship to R.A. We also thank Alper Atamtürk and Andrew Lim at the University of California, Berkeley for their advice and feedback.

[a]Author to whom correspondence should be addressed; electronic mail: ron@ieor.bankeley.edu

[1]National Center for Health Statistics, Prostate disease, Available: http://www.cdc.gov/nchs/fastats/prostate.htm, 2004.

[2]I.-C. J. Hsu, E. Lessard, V. Weinberg, and J. Pouliot, "Comparison of inverse planning simulated annealing and geometrical optimization for prostate high-dose-rate brachytherapy," Brachytherapy **3**, 147–152 (2004).

[3]E. Lessard and J. Pouliot, "Inverse planning anatomy-based dose optimization for HDR brachytherapy of the prostate using fast simulated annealing algorithm and dedicated objective function," Med. Phys. **28**, 773–779 (2001).

[4]E. Lessard, I.-C. J. Hsu, and J. Pouliot, "Inverse planning for interstitial gynecological template brachytherapy: Truly anatomy based planning," Int. J. Radiat. Oncol., Biol., Phys. **54**(5), 1243–1250 (2002).

[5]E. Lessard, "Development and clinical introduction of an inverse planning dose optimization by simulated annealing (IPSA) for high dose rate brachytherapy," Med. Phys. **31**(10), 2935 (2004).

[6]B. Lachance, D. Beliveau-Nadeau, E. Lessard *et al.*, "Early clinical experience with anatomy-based inverse planning dose optimization for high-dose-rate boost of the prostate," Int. J. Radiat. Oncol., Biol., Phys. **54**, 86–100 (2002).

[7]A. Mamoudieh, C. Tremblay, L. Beaulieu, B. Lachance, F. Harel, E. Lessard, J. Pouliot, and E. Vigneault, "Anatomy based inverse planning dose optimization in HDR prostate implant: A toxicity study," Radiother. Oncol. **75**, 318–324 (2005).

[8]D. Citrin, H. Ning, H. Guion, G. Li, R. C. Susil, R. W. Miller, E. Lessard, J. Pouliot, X. Huchen, J. Capala, C. N. Coleman, K. Camphausen, and C. Menard, "Inverse treatment planning based on MRI for HDR prostate brachytherapy," Int. J. Radiat. Oncol., Biol., Phys. **61**(4), 1267–1275 (2005).

[9]C. Ménard, R. C. Susil, P. Choyke, G. S. Gustafson, W. Kammerer, H. Ning, R. W. Miller, K. L. Ullman, N. S. Crouse, S. Smith, E. Lessard, J. Pouliot, V. Wright, E. McVeigh, C. N. Coleman, and K. Camphausen, "MRI-guided HDR prostate brachytherapy in a standard 1.5T scanner," Int. J. Radiat. Oncol., Biol., Phys. **59**(5), 1414–1423 (2004).

[10]K. D. DeWitt, I.-C. Hsu, V. K. Weinberg, E. Lessard, and J. Pouliot, "3-D inverse treatment planning for the tandem and ovoid applicator in cervical cancer," Int. J. Radiat. Oncol., Biol., Phys. **63**(4), 1270–1274 (2005).

[11]R. Taschereau, P. R. Stauffer, I.-C. Hsu, J. L. Schlorff, A. J. Milligan, and J. Pouliot, "Radiation dosimetry of a conformal heat-brachytherapy applicator," Technol. Cancer Res. Treat. **3**(4), 347–358 (2004).

[12]J. Pouliot, E. Lessard, and I.-C. J. Hsu, *Brachytherapy Physics*, 2nd ed. (Medical Physics Publishing, Madison, 2005).

[13]J. Pouliot, Y. Kim, E. Lessard, I.-C. Hsu, D. B. Vigneron, and J. Kurhanewicz, "Inverse planning for HDR prostate brachytherapy used to boost dominant intraprostatic lesions defined by magnetic resonance spectroscopy imaging," Int. J. Radiat. Oncol., Biol., Phys. **59**, 1196–1207 (2004).

[14]M. Lahanas, D. Baltas, and N. Zamboglou, "Anatomy-based three dimensional dose optimization in brachytherapy using multiobjective genetic algorithms," Med. Phys. **26**(9), 1904–1918 (1999).

[15]M. Lahanas, D. Baltas, and N. Zamboglou, "A hybrid evolutionary algorithm for multi-objective anatomy-based dose optimization in high dose rate brachytherapy," Phys. Med. Biol. **48**, 399–415 (2003).

[16]S. Geman and D. Geman, "Stochastic relation, Gibbs distribution and Bayesian restoration of images," IEEE Trans. Pattern Anal. Mach. Intell. **6**, 721–741 (1984).

[17]P. J. M. Van Laarhoven and E. H. L. Aarts, "Simulated annealing: Theory and applications," *Mathematics and Its Applications* (Reidel, Dordrecht, 1987).

[18]E. Aart and J. Korst, *Simulated Annealing and Boltzmann Machines*, Interscience Series in Discrete Mathematics and Optimization (Wiley, New York, 1989).

[19]Y. Yu, J. B. Zhang, G. Cheng, M. C. Schell, and P. Okunieff, "Multiobjective optimization in radiotherapy: Application to stereotactic radiosurgery and prostate brachytherapy," Artif. Intell. Med. **19**, 39–51 (2000).

[20]S. G. Nash and A. Sofer, *Linear and Nonlinear Programming* (McGraw-Hill, New York, 1996).

[21]W. D. Renner, T. P. O'Conner, and N. M. Bermudez, "An algorithm for generation of implant plans for high-dose-rate irradiators," Med. Phys. **17**, 35–40 (1990).

[22]P. Kneschaurek, W. Schiess, and R. Wehrmann, "Volume-based dose optimization in brachytherapy," Int. J. Radiat. Oncol., Biol., Phys. **45**, 811–815 (1999).

[23]G. Jozsef, O. E. Streeter, and M. A. Astrahan, "The use of linear programming in optimization of HDR implant dose distributions," Med. Phys. **30**, 751–760 (2003).

[24]M. Lahanas, D. Baltas, S. Giannouli, N. Milickovic, and N. Zamboglou, "Generation of uniformly distributed dose points for anatomy-based three-dimensional dose optimization methods in brachytherapy," Med. Phys. **27**, 1034–1046 (2000).

[25]R. Nath *et al.*, "Dosimetry of interstitial brachytherapy sources: Recommendations of the AAPM Radiation Therapy Committee Task Group No. 43," Med. Phys. **22**, 209–234 (1995).

[26]M. J. Rivard *et al.*, "Update of AAPM Task Group No. 43 Report: A revised AAPM protocol for brachytherapy dose calculations," Med. Phys. **31**, 633—674 (2004).

[27]R. G. Taylor, *Models of Computation and Formal Languages* (Oxford University Press, New York, 1998).

[28]R. Fourer, D. M. Gay, and B. W. Kernighan, *AMPL: A Modeling Language for Mathematical Programming*, 2nd ed. (Thomson/Brooks/Cole, Pacific Grove, CA, 2003).

[29]ILOG, Inc., ILOG CPLEX: High-performance software for mathematical programming and optimization, Available: http://www.ilog.com/products/cplex/, 2005.

[30]Y. Kim, S. M. Noworolski, J. Pouliot, I.-C. Hsu, D. B. Vigneron, and J. Kurhanewicz, "Expandable and rigid endorectal coils for prostate MRI: Impact on prostate distortion and rigid image registration," Med. Phys. **32**(12), 3569–3578 (2005).

[31]R. Alterovitz, K. Goldberg, J. Kurhanewicz, J. Pouliot, and I.-C. J. Hsu, "Image registration for prostate MR spectroscopy using biomechanical modeling and optimization of force and stiffness parameters," Proceedings of the 26th Annual International Conference of the IEEE Engineering In Medicine and Biology Society, San Francisco, CA, 2004, pp. 1722–1725.

[32]R. Alterovitz, K. Goldberg, J. Pouliot, I.-C. J. Hsu, Y. Kim, S. M. Noworolski, and J. Kurhanewicz, "Registration of MR prostate images with biomechanical modeling and nonlinear parameter estimation," Med. Phys. **33**(2), 446–454, (2006).